Clipping and Stoppering Anion Templated Synthesis of a [2]Rotaxane Host System

Yitong Li,[a] Kathleen M. Mullen,[a,c] João Sardinha,[b] Vítor Félix,[b] and Paul D. Beer*[a]

1. Synthesis of pyridinium axle derivatives

Toluene-4-sulfonic acid 2-(2-hydroxyethoxy)ethyl ester (5):

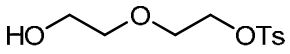

A solution of diethyleneglycol (4.24 g, 40.0 mmol), tosyl chloride (1.91 g, 10.0 mmol) and triethylamine (2.79 mL, 20.0 mmol) in dry dichloromethane (50 mL) was stirred under N_2 for one hour. After this time, the reaction mixture was washed with 1 M $KHSO_{4(aq)}$ (3 × 15 mL) and 5 % $NaHCO_{3(aq)}$ (3 × 15 mL) and dried over sodium sulfate. The solvent removed *in vacuo* and the residue was purified by column chromatography using 1:20 MeOH/CH_2Cl_2 as the elute to give the pure product as a clear colorless oil (1.93 g, 74 %); ^{1}H NMR (300 MHz, $CDCl_3$, 298 K): δ 7.80 (2H, d, ^3J = 8.1 Hz, Ar*H*), 7.35 (2H, d, ^3J = 8.1 Hz, Ar*H*), 4.19 (2H, t, OCH_2), 3.67 (4H, m, OCH_2), 3.52 (2H, t, OCH_2), 2.45 (3H, s, CH_3), 2.38 (1H, br t, O*H*); ^{13}C NMR (75 MHz, $CDCl_3$, 298 K): δ 145.0, 132.9, 129.8, 127.9, 72.5, 69.2, 68.5, 61.6, 21.6; ESI-MS (*m*/*z*): $[M + Na]^+$ 283.0614, $C_{11}H_{16}O_5SNa$ (calc. 283.0611).

***N*-(4-(2-(2-hydroxyethoxy)ethoxy)phenyl)acetamide (6):**

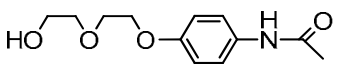

A solution of **5** (1.48 g, 6.60 mmol), *N*-(4-Hydroxy-phenyl)-acetamide (1.0 g, 6.6 mmol) and potassium carbonate (1.10 g, 7.9 mmol) in acetonitrile (50 mL) was refluxed under N_2 for 48 hours. After this time, the reaction mixture was then allowed to cool to room temperature, filtered and the solvent removed *in vacuo*. The residue was dissolved in chloroform (50 mL) and filtered through celite. The solvent was removed to give the pure product as a pale yellow oil (0.98 g, 72 %); ^{1}H NMR (300 MHz, $CDCl_3$, 298 K): δ 7.38 (2H, d, ^3J = 9.0 Hz, Ar*H*), 7.30 (1H, br s, -N*H*-), 6.86 (2H, d, ^3J = 9.0 Hz, Ar*H*), 4.12-4.09 (2H, m, -CH_2-), 3.86-3.83 (2H, m, -CH_2-), 3.78-3.74 (2H, m, -CH_2-), 3.69-3.65 (2H, m, -CH_2-), 2.14 (9H, s, -CH_3); ^{13}C NMR (125 MHz, $CDCl_3$, 298 K): δ

168.5, 155.7, 131.5, 122.1, 115.2, 72.8, 69.9, 67.9, 62.0, 24.6; ESI-MS (*m*/*z*): [M + Na]$^+$ 262.1053, $C_{12}H_{17}NO_4Na$ (calc. 262.1050).

2-(2-(4-Aminophenoxy)ethoxy)ethanol (7):

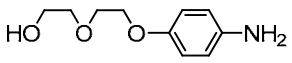

A solution of **6** (1.94 g, 8.10 mmol) and excess sodium hydroxide (6.60 g, 0.165 mol) in 5:1 H_2O/EtOH (120 mL) was refluxed under N_2 for 24 hours. After this time, the reaction mixture was allowed to cool room temperature, filtered and the solvent removed in *vacuo*. The residue was dissolved in water (100 mL) and extracted with dichloromethane (3 × 100 mL). The combined organic layers were dried over magnesium sulfate and the solvent removed to give the pure product as a white crystalline solid (1.10 g, 69 %); ^{1}H NMR (300 MHz, $CDCl_3$, 298 K): δ 6.79-6.74 (2H, m, Ar*H*), 6.66-6.61 (2H, m, Ar*H*), 4.08-4.05 (2H, m, -C*H*$_2$-), 3.84-3.81 (2H, m, -C*H*$_2$-), 3.77-3.73 (2H, m, -C*H*$_2$-), 3.69-3.66 (2H, m, -C*H*$_2$-), 2.95 (2H, br s, -N*H*$_2$); ^{13}C NMR (75 MHz, $CDCl_3$, 298 K): δ 151.8, 140.3, 116.4, 115.9, 72.5, 69.9, 68.2, 61.8; ESI-MS (*m*/*z*): [M + H]$^+$ 220.0948, $C_{10}H_{15}NO_3Na$ (calc. 220.0944).

4,4'-((4-Isocyanatophenyl)(phenyl)methylene)bis(*tert*-butylbenzene) (15):

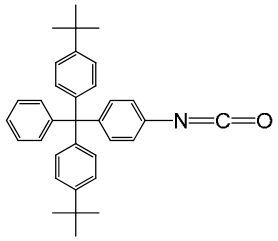

A solution of **14**[1] (0.133 g, 0.298 mmol), triphosgene (0.0530 g, 0.178 mmol) and triethylamine (0.0230 mL, 0.312 mmol) in toluene (50 mL) was heated at 70 ^{0}C under N_2 for 5 hours. After this time the reaction mixture was allowed to cool to room temperature and filtered. The solvent was removed *in vacuo* to yield an off white solid which was used immediately in the next step without any further purification or characterisation.

2. Characterisation

The high resolution ESI mass spectrum and isotopic modeling of [**3**]$^+$ is shown in Figure S1.

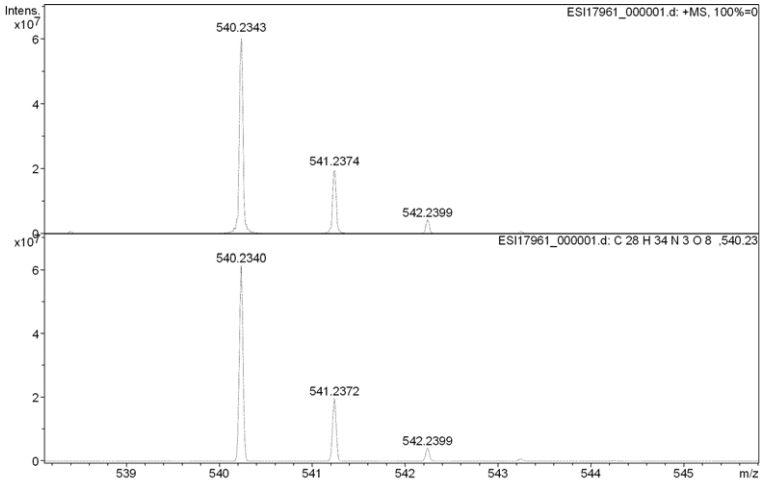

Figure S1 ESI MS (top) and isotopic modeling (bottom) of $[\mathbf{3}]^+$.

The high resolution ESI mass spectrum and isotopic modeling of $[\mathbf{4}]^+$ is shown in Figure S2.

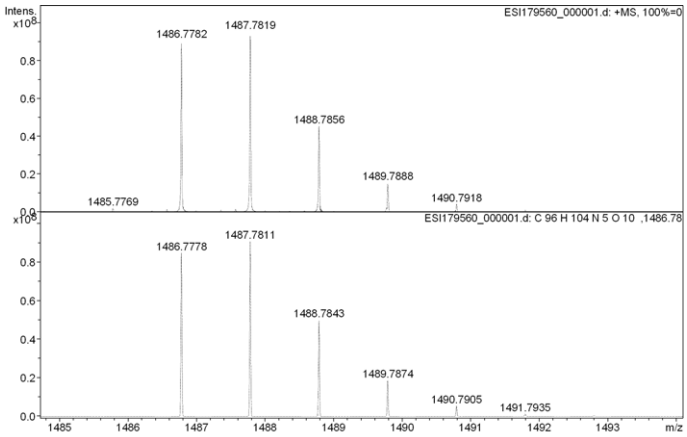

Figure S2 ESI MS (top) and isotopic modeling (bottom) of $[\mathbf{4}]^+$.

The high resolution ESI mass spectrum and theoretical isotope model of $[\mathbf{11}]^+$ is shown in Figure S3. The cationic peaks at m/z 2109.0201 agree well with the calculated value of 2109.0133.

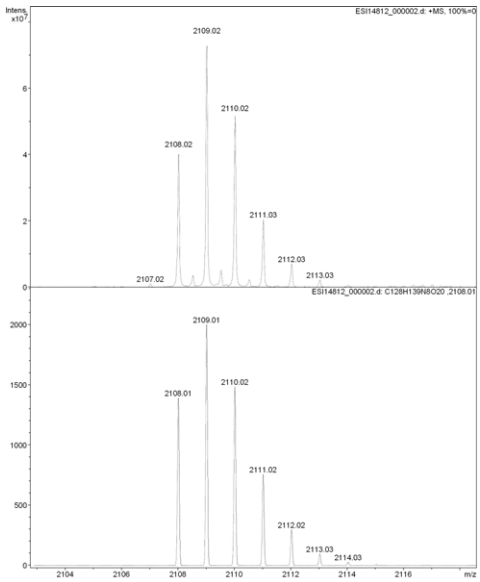

Figure S3 ESI MS (top) and isotopic modeling (bottom) of $[\mathbf{11}]^{+}$.

The full ^{1}H NMR spectrum of **11**-PF_6 and **11**-Cl are shown in Figure S3 and Figure S4 respectively.

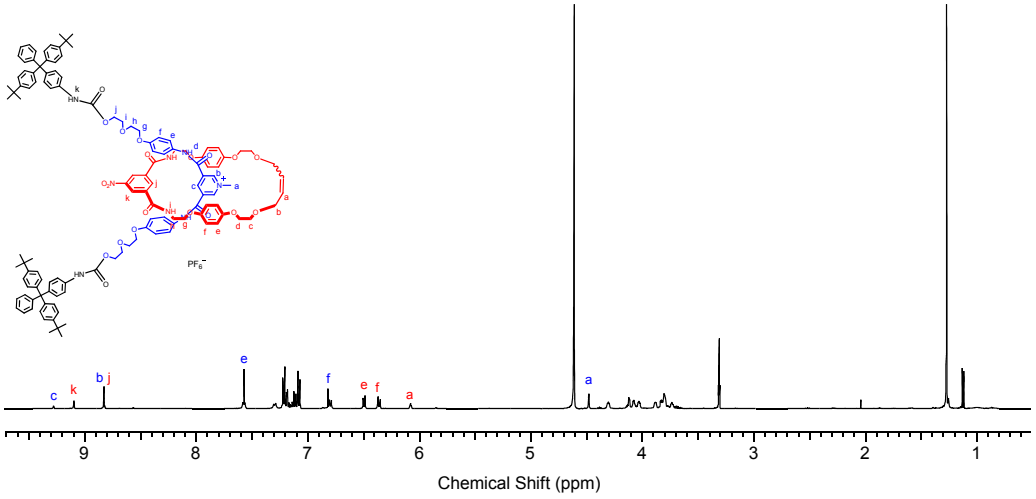

Figure S5 ^{1}H NMR (300 MHz, 298 K, 1:1 $CD_3OD/CDCl_3$) spectra of **11**-PF_6.

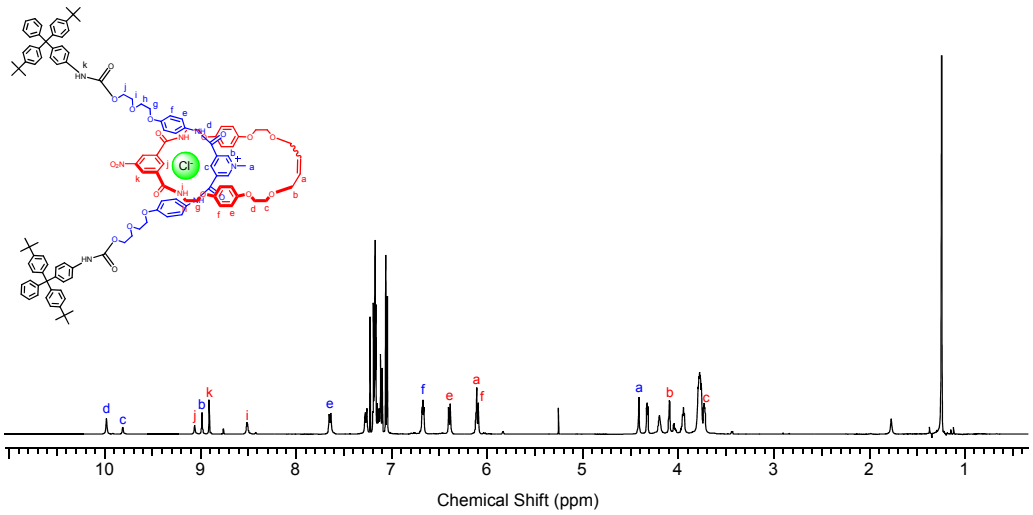

Figure S5 ^{1}H NMR (300 MHz, 298 K, 1:1 $CD_3OD/CDCl_3$) spectra of **11**-Cl.

3. Anion binding studies of macrocycle, axle and rotaxane

Preliminary ^{1}H NMR titration experiments of macrocycle **2** and axle **4**-BF_4 with anions were investigated in the competitive solvent mixtures 1:1 $CD_3OD/CDCl_3$ and 45:45:10 $CD_3OD/CDCl_3/D_2O$.[2] Typically, upon addition of anions, downfield perturbations of macrocycle nitro-aryl protons and axle pyridinium protons were observed which are indicative of anion complexation. Downfield shifts of amide protons can not be monitored in both cases due to the amide protons exchanging with deuterated solvent. For example, the titration spectra of **4**-BF_4 with TBACl in 1:1 $CD_3OD/CDCl_3$ are shown in Figure S5. Downfield shifts of pyridinium protons H_c and H_b were observed due to the coordination of the halide anion to the pyridinium amide cleft. As expected the pyridinium proton H_c exhibited the largest downfield shift.

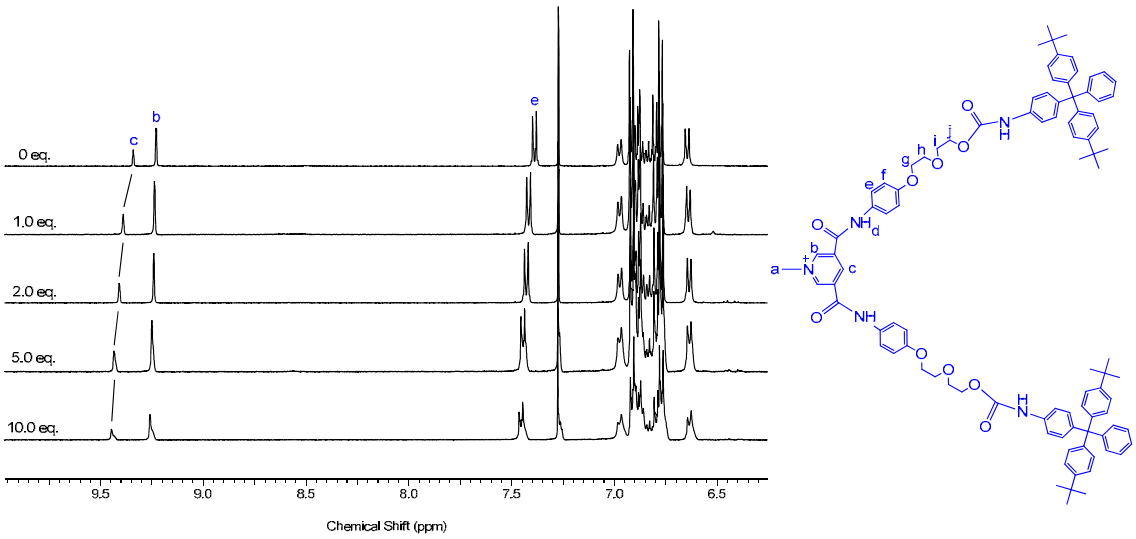

Figure S5 ^{1}H NMR (300 MHz, 298 K, 1:1 $CD_3OD/CDCl_3$) spectra of **4**-BF_4 with 0.0, 1.0, 2.0, 5.0 and 10.0 molar equivalents of TBACl.

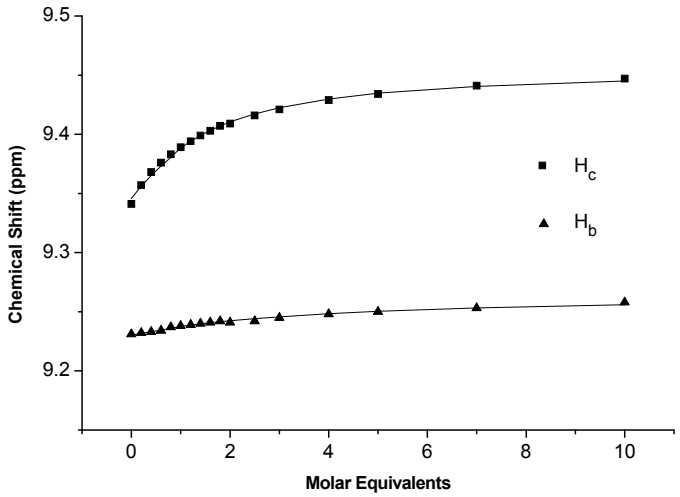

Figure S6 Titration curves of pyridinium protons H_b and H_c of **4**-BF_4 with TBACl in 1:1 $CD_3OD/CDCl_3$ at 298 K

Job plot analysis revealed 1:1 host/anion stoichiometry in all cases. WinEQNMR was used to determine association constants by analysis of the titration data of *para*-aryl proton H_j of macrocycle **2** and *para*-pyridinium proton H_c of axle **4**-BF_4.[2] Table 3.1 shows that positively charged axle **4**-BF_4 can bind anions more strongly than neutral macrocycle **2** due to favourable electrostatic interactions. It is noteworthy that both receptors exhibit stronger complexation with AcO^- anion in comparison to the less

basic halide anion binding. As expected anion binding affinities of both receptors decrease significantly from 1:1 $CD_3OD/CDCl_3$ to 45:45:10 $CD_3OD/CDCl_3/D_2O$. For example, axle **4**-BF_4 complexes chloride with a large association constant of K_a = 475 M^{-1} in 1:1 $CD_3OD/CDCl_3$ whereas the value diminishes to 140 M^{-1} in 45:45:10 $CD_3OD/CDCl_3/D_2O$. No complexation evidence of **2** with anions was observed in the aqueous solvent mixture.

4. ^{1}H NMR titration protocols

All NMR titration experiments were conducted on an Oxford Instruments Varian Unity Plus 500 MHz spectrometer, at 298 K. Initial sample volumes were 600 μL. The starting concentration of the host was 2 mM for all titrations. All anions were added as their TBA salts (0.06 M in 1.0 mL). 17 aliquots of the TBAX solutions (corresponding to 0, 0.2, 0.4, 0.6, 0.8, 1.0, 1.2, 1.4, 1.6, 1.8, 2.0, 2.5, 3.0, 4.0, 5.0, 7.0, 10.0 equivalents of added guest) were added until a total of 10 equivalents of the anion had been added. Spectra were recorded after each addition, and the sample shaken thoroughly before measurement.

Stability constants were obtained by analysis of the resulting titration data using the WinEQNMR[2] computer program. The various parameters were refined by non-linear least-squares analysis to achieve the best fit between observed and calculated chemical shifts. Comparison of the calculated binding isotherm with that obtained experimentally demonstrated that the model used was appropriate.

5. Molecular Modeling studies

All molecular dynamics (MD) simulations were carried out with the AMBER 11 suite of programs.[3] The individual components of the **11**$^+$ rotaxane system and the polyatomic anions were described with default Amber Force Field (GAFF)[4] with following exceptions:

Preliminary gas phase molecular mechanic (MM) calculations revealed that the default potential energy barrier (V_n) of 0.3 kcal for the X-*ca*-*na*-X torsion angle (where *ca* and *na* are the atom types assigned to the pyridinium ring carbon atoms and nitrogen

atom, respectively, and X means any other atom type) led to a slight bending of the *N*-methyl group of the pyridinium axle from the aromatic ring plane. This structural inaccuracy was corrected using the torsion force field parameters available in the GAFF for the related X-*cd*-*na*-X torsion angle (4 6.8 180.0 2), where *cd* is a sp^2 carbon in non-pure aromatic systems. The O-H hydrogen atoms of $H_2PO_4^-$ were assigned with non-default GAFF atom type *hx* in order to avoid the clash of the hydrogen atoms caused by the absence of van der Waals parameters for the default atom type *ho*.

Partial atomic charges of the individual components of the interlocked structure (macrocycle **2** and pyridinium axle) were RESP charges calculated at HF/6-31G* level as follows: the atomic coordinates of the macrocycle were generated from the structure taken from the X-ray single crystal of a pseudo-rotaxane system[5] by replacing the methyl group of the isophthalamide cleft by a nitro group. Afterwards, the structure was optimized *via* HF/6-31G* method and the electrostatic potential was calculated at the same level of theory using the Gaussian[6] IOP (6/33=2, 6/41=4, 6/42=6), as reported in the original force field publication.[4] The SO_4^{2-} charges were calculated using an equivalent methodology from a previous optimized structure at HF/6-31++G* level. To the best of our knowledge, the 3-D structure of the pyridinium axle was not available in any structural data base and taking account its flexibility the charges were derived through multi-conformation RESP fitting on the electrostatic potential of five HF/6-31G* previously optimized structures. The charges of AcO^- and $H_2PO_4^-$ anions were also RESP charges calculated at the same level of theory and they were obtained directly from the references [7] and [8] respectively.

The solvent molecules were described using a full atom model with atomic charges and force field parameters taken directly from the AMBER 11 software package for the methanol and TIP3P water,[9] except for chloroform whose parameters were taken from ref. [10]. The halide anions with charge of –1 were described using van der Waals parameters obtained from ref. [11].

The docking between $\mathbf{11}^+$ rotaxane system and anions Cl^-, OAc^-, $H_2PO_4^-$ and SO_4^{2-} was performed in gas phase through MD simulations at 2000 K. The individual interlocked **11**-anion associations were subjected to a 2 ns MD run using an integration

time step length of 1 fs. The use of this high temperature enables the system to cover all the conformational space since the energetic barriers are easily surmounted. 20000 structures were saved and subsequently energy minimized *via* MM. A representative structure of the more populated rotaxane-anion association cluster was solvated *via* PACKMOL[12] with a cubic box containing a random distribution composed of 750 chloroform, 1500 methanol and 750 water molecules, consistent with the v/v $CHCl_3/CH_3OH/H_2O$ (45:45:10) solvent mixture ratio. The charge neutrality of the **11**-SO_4^{2-} solvated system was achieved by addition of one tetrabutylammonium cation described with RESP charges and GAFF parameters. Subsequently, each solvated system was equilibrated under periodic boundary conditions using the following multi-stage protocol: minimization of the solvent molecules by MM keeping the solute fixed with a positional restrain of 500 kcal mol^{-1} $Å^{-2}$ followed by the relaxing of the entire system after restrain removal. The system was then heated up to 300 K for 50 ps using a NVT ensemble and a weak positional restraint (10 mol^{-1} $Å^{-2}$) on the solute. The positional restraint was then removed and the system was allowed to equilibrate in a NPT ensemble at 300 K for 500 ps. The system density remained constant during the last 300 ps of the MD equilibration run with a cubic box with edges dimension size of 61 Å. NPT data production runs (300 K, 1 atm) were carried out for 15 ns and the snapshots were saved to a trajectory file every 0.2 ps. Bond lengths involving all bonds to hydrogen atoms were constrained with the SHAKE algorithm[13] allowing to use a 2 fs time step. The Particle Mesh Ewald method[14] was used to treat the long-range electrostatic interactions and the non-bonded van der Waals interactions were truncated with a 12 Å cut-off. The collected data were analyzed with the PTRAJ module as implemented in the AMBER. The molecular diagrams were drawn with PyMOL.[15]

References

[1] Gibson, H. W.; Lee, S. H.; Engen, P. T.; Lecavalier, P.; Sze, J.; Shen, Y. X.; Bheda, M. *J. Org. Chem.* **1993**, 58, 3748-3756.

[2] Hynes, M. J. *J. Chem. Soc., Dalton Trans.* **1993**, 311-312.

[3] Case, D. A.; Darden, T. A.; Cheatham III, T. E.; Simmerling, C.; Wang, J.; Duke, R. E.; Luo, R.; Walker, R. C.; Zhang, W.; Merz, K. M.; Roberts, B. P.; Hayik, S.; Roitberg, A.; Seabra, G.; Kolossváry, I.; Wong, K. F.; Paesani, F.; Vanicek, J.; Liu, J.; Wu, X.; Brozell, S. R.; Steinbrecher, T.; Gohlke, H.; Cai, Q.; Ye, X.; Wang, J.; Hsieh, M.-J.; Hornak, V.; Cui, G.; Roe, D. R.; Mathews, D. H.; Seetin, M. G.; Sagui, C.; Babin, V.; Luchko, T.; Gusarov, S.; Kovalenko, A.; Kollman, P. A. AMBER 11, University of California, San Francisco, 2010.

[4] Wang, J.; Wolf, R. M.; Caldwell, J. W.; Kollman, P. A.; Case, D. A. *J. Comput. Chem.* **2004**, *25*, 1157–1174.

[5] Sambrook, M. R.; Beer, P. D.; Wisner, J. A.; Paul, R. L.; Cowley, A. R.; Szemes, F.; Drew, M. G. B. *J. Am. Chem. Soc.* **2005**, *127*, 2292-2302.

[6] Gaussian 03, Revision C.02, Frisch, M. J.; Trucks, G. W.; Schlegel, H. B.; Scuseria, G. E.; Robb, M. A.; Cheeseman, J. R.; Montgomery, Jr., J. A.; Vreven, T.; Kudin, K. N.; Burant, J. C.; Millam, J. M.; Iyengar, S. S.; Tomasi, J.; Barone, V.; Mennucci, B.; Cossi, M.; Scalmani, G.; Rega, N.; Petersson, G. A.; Nakatsuji, H.; Hada, M.; Ehara, M.; Toyota, K.; Fukuda, R.; Hasegawa, J.; Ishida, M.; Nakajima, T.; Honda, Y.; Kitao, O.; Nakai, H.; Klene, M.; Li, X.; Knox, J. E.; Hratchian, H. P.; Cross, J. B.; Bakken, V.; Adamo, C.; Jaramillo, J.; Gomperts, R.; Stratmann, R. E.; Yazyev, O.; Austin, A. J.; Cammi, R.; Pomelli, C.; Ochterski, J. W.; Ayala, P. Y.; Morokuma, K.; Voth, G. A.; Salvador, P.; Dannenberg, J. J.; Zakrzewski, V. G.; Dapprich, S.; Daniels, A. D.; Strain, M. C.; Farkas, O.; Malick, D. K.; Rabuck, A. D.; Raghavachari, K.; Foresman, J. B.; Ortiz, J. V.; Cui, Q.; Baboul, A. G.; Clifford, S.; Cioslowski, J.; Stefanov, B. B.; Liu, G.; Liashenko, A.; Piskorz, P.; Komaromi, I.; Martin, R. L.; Fox, D. J.; Keith, T.; Al-Laham, M. A.; Peng, C. Y.; Nanayakkara, A.; Challacombe, M.; Gill, P. M. W.; Johnson, B.; Chen, W.; Wong, M. W.; Gonzalez, C.; Pople, J. A. Gaussian, Inc., Wallingford CT, 2004.

[7] Meng, E.C.; Cieplak, P.; Caldwell, J. W.; Kollman, P. A. *J. Am. Chem. Soc.* **1994**, *116*(26), 12061–12062.

[8] Blas, J. R.; Márquez, M.; Sessler, J. L.; Luque, F. J.; Orozco, M. *J. Am. Chem. Soc.* **2002**, *124*, 12796-12805.

[9] Jorgensen, W. L.; Chandrasekhar, J.; Madura, J. D.; Impey, R. W.; Klein, M. L. *J. Chem. Phys.* **1983**, *79*, 926 – 935.

[10] Fox, T.; Kollman, P. A. *J. Phys. Chem. B* **1998**, *102*, 8070–8079.

[11] Joung, I. S.; Cheatham III, T. E. *J. Phys. Chem. B* **2008**, *112*, 9020-9041.

[12] Martínez, L.; Andrade, R. Birgin, E. G.; Martínez, J. M. *J. Comput. Chem.* **2009**, *30*(13), 2157-2164.

[13] Ryckaert, J. P.; Cicotti, G.; Berendsen, H. J. C. *J. Comput. Phys.* **1977**, *23*, 327-342.

[14] Essmann, U.; Perera L.; Berkowitz, M. L.; Darden, T.; Lee, H.; Perdensen, L. G. *J. Chem. Phys.* **1995**, *103*, 8577-8593.

[15] The PyMOL Molecular Graphics System, Version 1.2r3pre, Schrödinger, LLC.